Vol. 05, No. 01, pp. 07 –12 (2024)
ISSN: 2709-6904

JoCEF

JOURNAL OF CIVIL ENGINEERING FRONTIERS

www.jocivilef.org

Performance Assessment of Mobile Laser Scanning Systems Using Velodyne Hdl-32e

Bashar Alsadik

Department of Earth Observation Science, ITC Faculty, University of Twente, The Netherlands, b.s.a.alsadik@utwente.nl

Abstract

Mapping systems using multi-beam LiDARs are widely used nowadays for different geospatial applications graduating from indoor projects to outdoor city-wide projects. These mobile mapping systems can be either ground-based or aerial-based systems and are mostly equipped with inertial navigation systems INS. The Velodyne HDL-32 LiDAR is a well-known 360° spinning multi-beam laser scanner that is widely used in outdoor and indoor mobile mapping systems. The performance of such LiDARs is an ongoing research topic which is quite important for the quality assurance and quality control topic. The performance of this LiDAR type is correlated to many factors either related to the device itself or the design of the mobile mapping system. Regarding design, most of the mapping systems are equipped with a single Velodyne HDL32 in a specific orientation angle which is different among the mapping systems manufacturers. The LiDAR orientation angle has a significant impact on the performance in terms of the density and coverage of the produced point clouds. Furthermore, during the lifetime of this multi-beam LiDAR, one or more beams may be defected and then either continue the production or returned to the manufacturer to be fixed which then cost time and money. In this paper, the design impact analysis of a mobile laser scanning (MLS) system equipped with a single Velodyne HDL-32E will be clarified and a clear relationship is given between the orientation angle of the LiDAR and the output density of points. The ideal angular orientation of a single Velodyne HDL-32E is found to be at 35° in a mobile mapping system. Furthermore, we investigated the degradation of points density when one of the 32 beams is defected and quantified the density loss percentage and to the best of our knowledge, this is not presented in literature before. It is found that a maximum of about 8% point density loss occurs on the ground and 4% on the facades when having a defected beam of the Velodyne HDL-32E.

Keywords: *Mobile mapping systems, LiDAR, Velodyne HDL-32, defected beams, quality control, 3D simulation, point density.*

Received: October 3rd, 2023 / Accepted: February 22nd, 2024 / Online: March 2nd, 2024

I. INTRODUCTION

LiDAR technology is witnessing significant progress nowadays motivated by the market needs of the industrial and mapping sectors, mainly for autonomous driving and the orientation toward smart city technologies [1-3]. Some LiDAR manufacturers already made a significant contribution and a worldwide reputation like Velodyne [4] with its multi-beam spinning types like HDL-64E, HDL-32E, VLP-16, and the Prime Alpha "Fig.1". Many other companies are lately entering this thriving LiDAR market with competitive scanning properties and prices like Ouster [5], Hesai [6], Luminar [7], and Blickfeld [8].

Fig.1. Different Velodyne multi-beam LiDAR types.

Velodyne LiDAR types are multi-beam (16, 32, 64, or 128 channels) spinning scanners at a high speed of 5-30 Hz with long ranges, centimeters range accuracy, multi returns, and

doi: 10.38094/jocef50177

reasonable vertical field of view VFOV. These aspects make Velodyne LiDAR types suitable and demanded devices for ground-based and aerial-based mobile mapping systems.

Among the mentioned types of Velodyne products, the HDL-32E type is the most used one in mobile mapping systems because of its high productivity and centimetric accuracy besides its adequate size, weight, and power consumption "Table I". Some mobile mapping systems using the HDL-32E LiDAR are shown in Fig.2 like Maverick [9], TOPCON [10], and Viametris [11].

a) b) c)

Fig. 2. Mobile mapping systems using Velodyne HDL-32E. a) Maverick. b) TOPCON. c) Viametris.

TABLE I. VELODYNE HDL-32E SPECIFICATIONS [12]

LiDAR Sensor	Velodyne HDL-32
Max. Range	≤ 100m
Range Accuracy 1σ	±2cm (Typical)
Beam divergence	0.16° (2.8mrad)
Beam footprint	28cm@100m
Output rate pts/sec.	≈700000
Points per revolution	35000 pts @ 20Hz
FOV - Vertical	≈ 41.33° (+10.7°: -30.7°)
Rotation rate	5-20 Hz
Vertical resolution	V:1.33°
Horizontal resolution	H:0.1°-0.4°
Pulse return	dual return
Number of beams	32 beams
Weight	1050g
Estimated price	≈$45K
Power consumption	12w

The angular orientation of the HDL-32E is different between the mapping systems and may ranges generally between 25˚-45˚. This angular orientation is governed by many design factors besides the required point density and coverage of the mapped features like roads and buildings [13, 14].

Furthermore, it can happen in the lifetime of the LiDARs that one or more beam channels are defective and no longer properly work. Accordingly, the mapping agencies probably return the defective LiDAR to the manufacturer to be fixed, but it will consume time and money. On the other hand, the mapping can be continued at the risk of having a degraded production quality than promised to clients.

Accordingly, in this paper, an analysis is applied to show the relation between the angular orientation of the HDL-32E LiDAR in an MLS system and the produced density of points. Furthermore, investigate the degradation amount of the density of points (density loss) when one of the 32 beams has defected and whether it is adequate to continue the mapping or not.

As mentioned, the HDL-32E is widely used for mobile mapping systems and it has 32 scanning beams with a wide VFOV of ≅40˚. The summarized specifications of this LiDAR is given in Table 1.

Fig. 3 shows the configuration of the 32 beams and the scanning patterns of the HDL-32E in a rectangular space when placed at the center of the space while the LiDAR is oriented at 0˚ in a stationary scan of one stationary scan revolution.

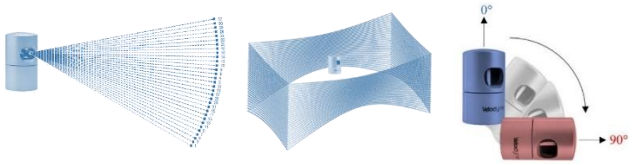

a) b) c)

Fig. 3. a) Scanning beam configuration of the HDL-32E. b) Scanning pattern illustration. c) Angular orientation of the LiDAR [15].

II. METHODOLOGY

The method adopted in this research is applied in two phases: 1) studying the impact of the angular orientation of the LiDAR on the produced density of points. 2) Assessing the impact of one beam defect in the performance.

To quantify the relation between the angular orientation of the HDL-32E and the produced point cloud, a simple simulated model is used as shown in Fig. 4 which consists of a 50 m width of a road and 70 m height of a building facade located at the side of the road. The scans are simulated for both features and the density is evaluated at every orientation angle graduating from 0˚ to 90˚ at an interval of 5˚. All the simulations and calculations are applied using a MATLAB code prepared by the author (Table II).

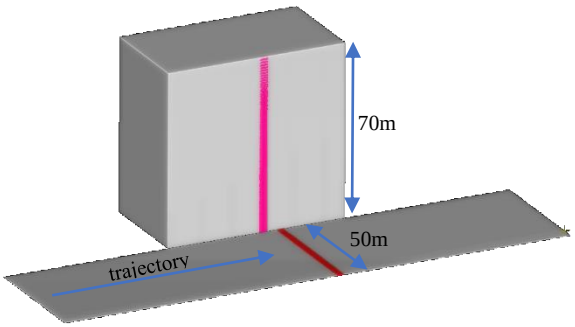

Fig.4. The simulated road and building façade and two selected slices for testing the point density.

Furthermore, to assess the beam deficiency impact, one beam is turned off each time at a selected orientation angle. A simulation scanning is applied assuming the LiDAR has one defected beam and the point density is calculated every time.

The algorithm of the proposed simulation method is shown in Table II as follows:

TABLE II ALGORITHM OF THE LIDAR DEFECTIVE BEAMS SIMULATION.

- Load the Velodyne beams angular configuration.
- Define the simulation objects by a mesh surface or planes.
- Define the LiDAR parameters and the path of the scanning.
- Apply the computations:
  For each beam j
  Turn off j – remaining 31 beams
  For each scanning station i on the planned path.
  For each scanning beam.
  For each scanning angle [0˚- angular resolution - 360˚].
  Apply the LiDAR equation [16] *using the predefined orientation using polar coordinates azimuth, elevation, and range.*
  Check if the calculated scanning ray is intersecting the mesh.
  Check visibility
  Save scanning point XYZ
  Repeat

Fig.5 shows the workflow methodology of this paper.

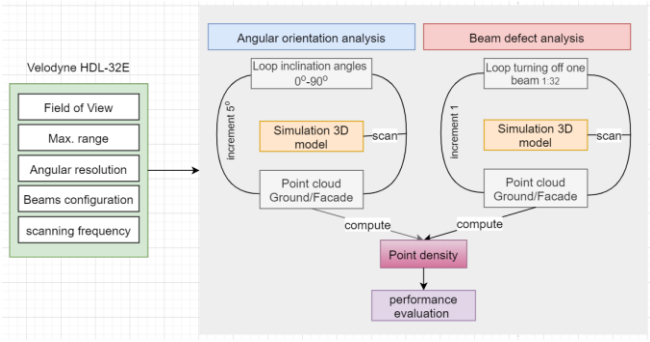

Fig. 5. Methodology workflow.

III. RESULTS

As mentioned in section 2, the orientation angle is incrementally changed from 0˚ to 90˚ in the scanning simulation of the model shown in Fig.4. The simulation is applied by intersecting the LiDAR beams with the road and the façade planes as mathematically described in [17].

For illustration, Fig. 6 shows the scanning patterns of points on the ground at the different angular orientations of the LiDAR for one stationary scanning sweep.

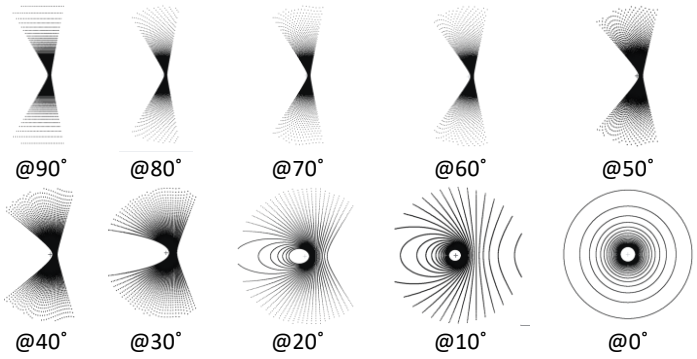

Fig.6. Scanning patterns on the ground using the Velodyne HDL-32E at different orientation angles.

As mentioned, the scanning simulation of the model in Fig.4 is applied, assuming an MLS system equipped with an HDL-32E LiDAR at a driving speed of 10 m/sec. and at 2 m height above the ground. Graphical plots explaining the relation between the produced point cloud and the LiDAR orientation angle are shown in Fig.7a and the relation between the point density and the LiDAR orientation angle is shown in Fig.7b.

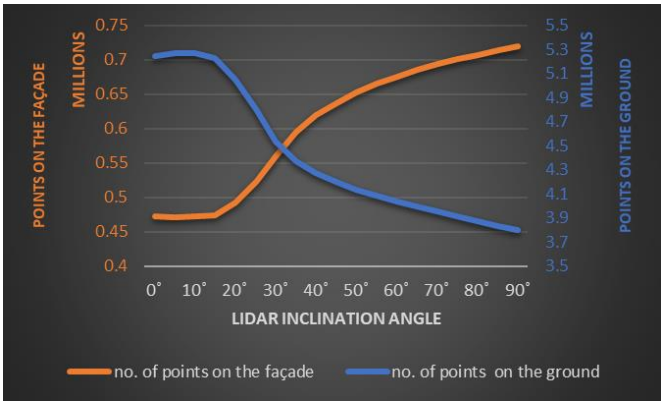

a)

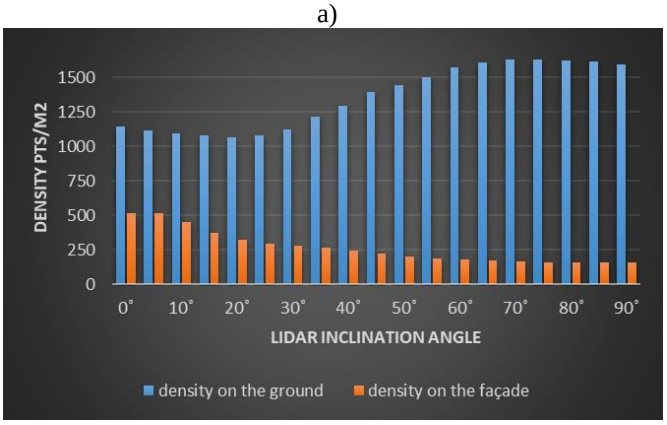

b)

Fig.7. a) The relation between the produced point cloud and the LiDAR orientation angle. b) The relation between the average point density and the LiDAR orientation angle.

Furthermore, the selected slices on the road surface and the facade "Fig.4" are used to visualize the density profile sections as shown in Fig.8. It should be noted that the mapping trajectory is assumed at the 0 x-axes in Fig.8a.

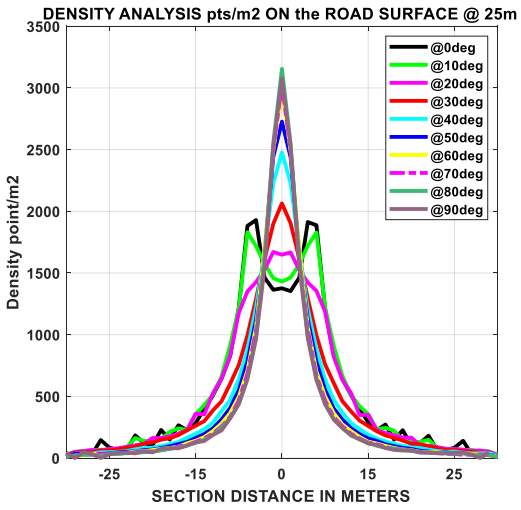

a)

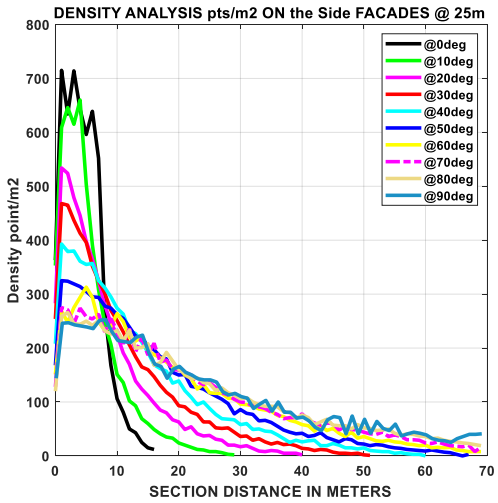

b)

Fig. 8. Point density profiles. a) At the road surface slice. b) At the side building façade slice.

To better illustrate the expected density of points and their distribution on relatively smaller objects, a simulation is applied on a scanned standing still person 10 meters aside from the vehicle trajectory. The results are illustrated in Fig. 9 which shows a clear relationship between the different LiDAR orientation angles and the density of points.

The second phase of this research is to investigate the impact of having one LiDAR beam defect on the final density of points "Fig.10". The scanning simulation is applied to the simple model shown in Fig.4 where the density of points is computed on the ground and the facade. Three orientation angles are selected arbitrarily to apply this task at 20˚, 30˚, and 45˚ respectively. The density loss is evaluated by dividing the degradation in the density when having one beam defect to the point density when the LiDAR is fully functional.

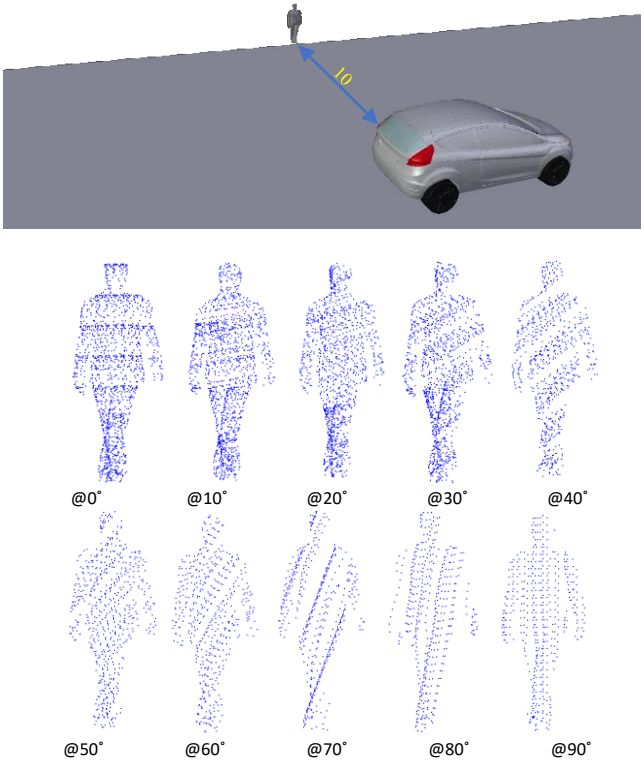

Fig.9. Point clouds of a standing person at different orientation angles of the LiDAR 10 meters aside from the mobile mapping vehicle trajectory.

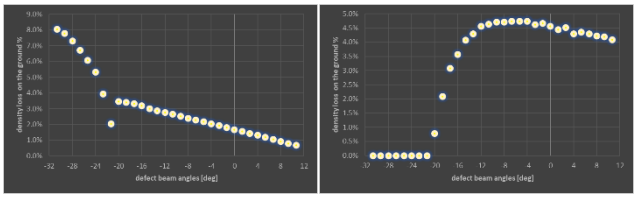

a)

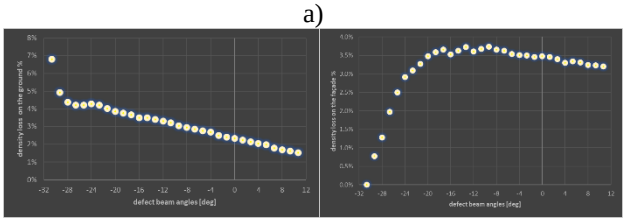

b)

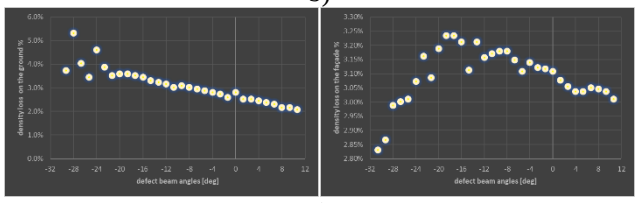

c)

Fig. 10. The density loss % of the 32 beams of the HDL-32E. Left) ground. Right) façade. a) At 20˚ orientation angle. b) At 30˚ orientation angle. c) At 45˚ orientation angle.

IV. Discussion

From the results shown in section 3, several observations can be listed as:

- There is an obvious relation between the number of scanned points and the LiDAR orientation angle. Whenever, the orientation angle increases, the number of points on the ground decreases, and on the facades increases "Fig.7a".
- Generally, whenever the orientation angle increases, the density of points on the ground increases, and on the facades decreases "Fig.7b". However, increasing the orientation angle has an impact on the coverage of the point cloud as well. Similarly, point densities shown in Fig.9 for a scanned standing still person decreased whenever the orientation angle increased. Furthermore, the uniformity of points distribution worsened.
- The density attained on facades is always less than the density on the ground in whatever orientation angle of the LiDAR. This is also related to the fact that buildings are always located at farther distances from the LiDAR than the ground beneath the driving vehicle.
- Whenever the orientation angle decreases, the point density related to the road width increases. As an example "Fig.8a", at a 20˚ angle, the density of points is >1000 pts/m^2 within 8 m width aside the mapping trajectory. While at 30˚, the density of ground points is >1000 pts/m2 within 6 m width aside the mapping trajectory. As mentioned, all these numbers are based on a simulation with a driving speed of 50 km/h.
- The beams which are oriented below the horizon, especially the ones having the following angular orientation of -24, -28, -29.33, and -30.67 are more significant on the ground density loss than the other beams. On the other hand, those mentioned LiDAR beams are the most insignificant on the façade density loss "Fig.10". This is logical since the mentioned beams are scanning the ground at shorter distances.
- The defected beams have a minor impact on the final point density, especially on facades. A maximum density, loss of 8% is found on the ground while a maximum of 4% is found on the facades.
- Finding the ideal angular orientation of the LiDAR is a complicated task and depending on the preference and the aims of the mapping. Mostly, mapping companies are aiming for a high density of points on the ground in the first place and then for building facades. To find a compromise between both it is suitable to select the orientation angle of 35˚ as it represents the intersection of the curves shown in Fig.5a. In this manner, the MLS system equipped with an HDL-32 is expected to produce a point cloud with an average point density of about 1200 pts/m^2 on the ground and 250 pts/m^2 on facades located 25 m aside from the mapping trajectory at 50 km/h speed.

V. Conclusions

Several leading mapping companies are using the Velodyne HDL-32E LiDAR as described in section 1. In this paper, the relation between the angular orientation of the HDL-32E LiDAR and the density of points is investigated. Furthermore, the quantification of the density loss is shown in case of one beam is defective out of the 32 beams.

Different factors are influencing the productivity of the mobile laser scanning MLS system. However, the angular orientation of the LiDAR is the most important because of its direct relation to the point cloud productivity in terms of coverage and density.

The results showed a clear relationship between the angular orientation of the LiDAR and the density of points on the ground and the side facade "Fig.7". As a compromise to have an adequate point cloud density on both features, the orientation angle at 35˚ is recommended.

In the same context, the impact of having one beam defect of the HDL-32E is analyzed as shown in Fig.10. It is concluded that one beam defect is insignificant in terms of density loss on the ground or facade features. A maximum density loss is found to be around 8% on the ground and 4% on the façade. However, this is not yet verified for other features like poles, trees, electricity cables, etc., and will be investigated in future work. Moreover, to investigate the outcome of the LiDAR when the laser beams have defected in a successive scenario. Other state-of-the-art LiDAR devices will be investigated in the future to evaluate their performance and productivity.

References

[1] R. Santiago and B.-G. Maria, "An Overview of Lidar Imaging Systems for Autonomous Vehicles," *Applied Sciences*, vol. 9, no. 19, p. 4093, 2019.

[2] R. Shanker, A. Jonas, S. Devitt, K. Huberty, S. Flannery, and W. Greene, "Autonomous Cars: Self-Driving the New Auto Industry Paradigm," 2013. [Online]. Available: https://studylib.net/doc/8717560/autonomous-cars--self-driving-the-new-auto-industry-paradigm

[3] R. Garnett and M. Adams, "LiDAR—A Technology to Assist with Smart Cities and Climate Change Resilience: A Case Study in an Urban Metropolis," *ISPRS International Journal of Geo-Information*, vol. 7, p. 161, 04/24 2018, doi: 10.3390/ijgi7050161.

[4] Velodyne. https://velodynelidar.com/ (accessed 1 October, 2018).

[5] Ouster. https://ouster.com/ (accessed November 2018, 2018).

[6] Hesai. https://www.hesaitech.com/en/ (accessed August 2019, 2019).

[7] Luminar. https://www.luminartech.com/ (accessed July 2019, 2019).

[8] Blickfeld. https://www.blickfeld.com/ (accessed July 2019, 2019).

[9] "Maverick." https://www.teledyneoptech.com/en/products/mobile-survey/maverick/ (accessed July 2020).

[10] TOPCON. "IP-S3 mobile mapping system." https://www.topconpositioning.com/mass-data-and-volume-collection/mobile-mapping/ip-s3 (accessed July 21, 2020).

[11] Viametris. "vMS3D." https://www.viametris.com/vms3d (accessed July 21, 2020).

[12] Velodyne. "HDL-32E. High Resolution Real-Time 3D Lidar Sensor." https://velodynelidar.com/products/hdl-32e/ (accessed 20 th of August 2020).

[13] S. Oh, J.-H. You, A. Eskandarian, and Y.-K. Kim, *Accurate Alignment Inspection System for Low-resolution Automotive and Mobility LiDAR*. 2020.

[14] T. Knaak, "Establishing Requirements, Extracting Metrics and Evaluating Quality of LiDAR Data ", USA, 2015. [Online]. Available: https://new.certainty3d.com/blog/wp-content/uploads/2018/01/TopoDOT_TechNote_1021_Requirements_Metrics_QB.pdf

[15] B. Alsadik, "Ideal angular orientation of selected 64-channel multi beam Lidars for mobile mapping systems," *Remote sensing*, vol. 12, no. 3, pp. 1-20, 2020, doi: https://doi.org/10.3390/rs12030510.

[16] S. J. Gordon and D. D. Lichti, "Terrestrial Laser Scanners with A Narrow Field of View: The Effect on 3D Resection Solutions," *Survey Review*, vol. 37, no. 292, pp. 448-468, 2004/04/01 2004, doi: 10.1179/sre.2004.37.292.448.

[17] B. Alsadik and F. Remondino, "Flight Planning for LiDAR-Based UAS Mapping Applications," *ISPRS Int. J. Geo-Inf.*, vol. 9, no. 6, p. 378, 2020. https://doi.org/10.3390/ijgi9060378